
Article:
Smith, L. orcid.org/0000-0002-5480-4392, Ibn-Mohammed, T., Yang, F. et al. (3 more authors) (2019) Comparative environmental profile assessments of commercial and novel material structures for solid oxide fuel cells. Applied Energy, 235. pp. 1300-1313. ISSN 0306-2619

https://doi.org/10.1016/j.apenergy.2018.11.028

Applied Energy 235 (2019) 1300–1313

Contents lists available at ScienceDirect

Applied Energy

journal homepage: www.elsevier.com/locate/apenergy

Comparative environmental profile assessments of commercial and novel material structures for solid oxide fuel cells

Lucy Smith[a,*], Taofeeq Ibn-Mohammed[b,c,*], Fan Yang[a], Ian M. Reaney[a], Derek C. Sinclair[a], S.C. Lenny Koh[b,c]

[a] Department of Materials Science & Engineering, The University of Sheffield, Sheffield S1 3JD, UK
[b] Centre for Energy, Environment & Sustainability, The University of Sheffiled, Sheffield S10 1FL, UK
[c] Advanced Resource Efficiency Centre, The University of Sheffield, Sheffield S10 1FL, UK

HIGHLIGHTS

- Comparative environmental impacts of novel and commercial SOFCs was conducted.
- Novel structures show lower environmental impact than the commercial counterparts.
- Electricity is the highest impact of novel SOFCs; higher than commercial structures.
- A number of intervention options for energy reduction are specified.

GRAPHICAL ABSTRACT

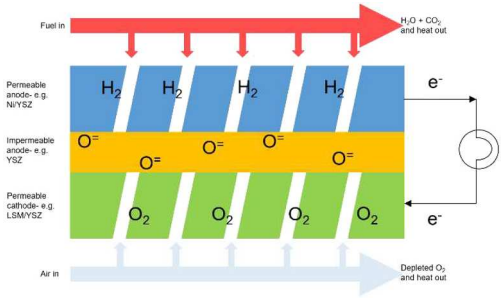

ARTICLE INFO

Keywords:
Climate change
Life cycle assessment
Solid oxide fuel cells
Materials efficiency
Functional materials
Energy

ABSTRACT

Globally, the issue of climate change due to greenhouse gas (GHG) emissions is now broadly acknowledged as one of the major challenges facing humankind that requires urgent attention. Accordingly, considerable efforts on clean energy technologies and policy recommendations have been developed to address this challenge. Solid oxide fuel cells (SOFCs) have been touted to play a role in achieving a reduction in global GHG emissions, offering numerous advantages including higher efficiencies and reduced emissions, over other conventional methods of energy generation. The increasing recognition and emphasis on fuel cells as a representative power generation system of the future has raised concerns over their environmental profile. Extensive research regarding the environmental profile of current structures of SOFCs can be found in the literature, but none consider the use of new materials to achieve lower environmental impacts. This research fills the gap and presents a comparison of the environmental profile of three SOFC structures: a commercially available structure, and two intermediate temperature structures, one using erbia-stabilised bismuth oxide electrolytes and a proposed structure using strontium-doped sodium bismuth titanate electrolytes. Using a functional unit of kg/100 kW of power output for each of the SOFC structures (excluding the interconnects), within a hybrid life cycle analysis framework, the environmental hotspots across the supply chains of each SOFC type are identified, quantified and ranked. The results show the use of these novel material combinations leads to a reduction in embodied materials and toxicological impact but higher electrical energy consumption during fabrication, in comparison to commercial SOFCs. The findings support the move to reduce the operating temperatures of SOFCs using these novel material architectures, which leads to an overall reduction in environmental impact due to the lower operational energy requirement of the chosen material constituents.

* Corresponding authors at: Centre for Energy, Environment & Sustainability, The University of Sheffiled, Sheffield S10 1FL, UK (T. Ibn-Mohammed); Department of Materials Science and Engineering, The University of Sheffield, Sheffield, S13 JD, UK (L. Smith).
E-mail addresses: lsmith17@sheffield.ac.uk (L. Smith), t.ibn-mohammed@sheffield.ac.uk (T. Ibn-Mohammed).

https://doi.org/10.1016/j.apenergy.2018.11.028
Received 19 June 2018; Received in revised form 2 November 2018; Accepted 9 November 2018
Available online 26 November 2018

Nomenclature

Acidification potential AP
Cumulative energy demand CED
Di-n butyl phthalate DBP
Energy payback period EPP
Environmental input-output EIO
Erbia-stabilised bismuth oxide ESB
Eutrophication potential EP
Freshwater aquatic ecotoxicity potential FAETP
Freshwater sediment ecotoxicity potential FSETP
Gadolinium doped ceria GDC
Global warming potential GWP
Greenhouse gas GHG
Human toxicity potential HTP
Life cycle assessment LCA
Marine aquatic ecotoxicity potential MAETP
Marine sediment ecotoxicity potential MSETP
Platinum group metal PGM
Polyethylene glycol PEG
Polyvinyl butral PVB
Pulsed laser deposition PLD
Rare earth oxides REO
Solid oxide fuel cell SOFC
Strontium-doped lanthanum manganite LSM
Strontium-doped sodium bismuth titanate NBT
Supply Chain Environmental Assessment Tool-intelligence SCEnATi
Yttrium stabilised zirconia YSZ

1. Introduction

In a world where rising energy demand competes with calls for green, sustainable energy to reduce the threat of climate change [1], the fuel cell presents a promising alternative to the combustion process for fuel production. Solid Oxide Fuel Cells (SOFCs) convert fuel to energy through electrochemical reactions at high efficiencies rather than the conventional combustion process, given that their efficiencies are not restricted by the Carnot cycle of a heat engine [2]. SOFCs are efficient, reduce carbon dioxide emissions in comparison to conventional methods and eliminate the emissions of other pollutants such as NO_x and SO_x altogether [3–5]. They have the potential to reach efficiencies of over 85% (lower heating value- LHV) in combined heat and power applications [6] and are currently in use as auxiliary power units for trucks and cars and in military applications [7]. As such, they are regarded as one of the cleanest power generation technologies with less impact on the natural environment [8].

A SOFC is composed of three essential parts: a porous cathode, a porous anode and an impermeable electrolyte. Their operating temperature is dictated by the temperature required by the electrolyte to achieve the necessary ionic conductivity in order to function [9]. The most common electrolyte material is yttrium stabilised zirconia (YSZ) which has high conductivity above 800 °C, negligible electronic conductivity between 800 and 1500 °C as well as chemical stability and mechanical strength [2]. A popular cathode material is a strontium-doped lanthanum manganite (LSM) and yttria-stabilised zirconia (YSZ) composite and anodes are often composed of nickel oxide-YSZ [10]. With an operating temperature range of 800–1000 °C, these commercial SOFCs undergo thermal stresses during their cycle of operation and this often leads to catastrophic failure. Furthermore, these high operating temperatures require ceramic interconnects which are expensive and must undergo complex manufacturing processes [10]. Fig. 1 provides a pictorial representation of the operating principle of a SOFC.

Current SOFC development is focused on reducing the cost of manufacturing, increasing the in-service lifespan and lowering operating temperatures through the synthesis of alternative materials [3,11]. Reduced operation temperatures also lead to difficulties such as increased resistance of the electrolyte and reduced reactions rates which in turn lead to reduced voltage and output [11]. These issues are being overcome through the use of novel cathode, electrolyte and anode materials. Compounds such as erbia-stabilised bismuth oxide (ESB), gadolinium doped ceria (GDC) and strontium-doped sodium bismuth titanate (NBT) are proposed for electrolyte manufacturing. In addition, cathodes composed of bismuth ruthenate-bismuth oxide and NBT stabilised with iron oxide are under investigation and anodes such as nickel oxide with GDC show promise [6,12].

While a push for a reduction in the operating temperature of SOFCs is necessary to achieve cost and energy savings and to improve

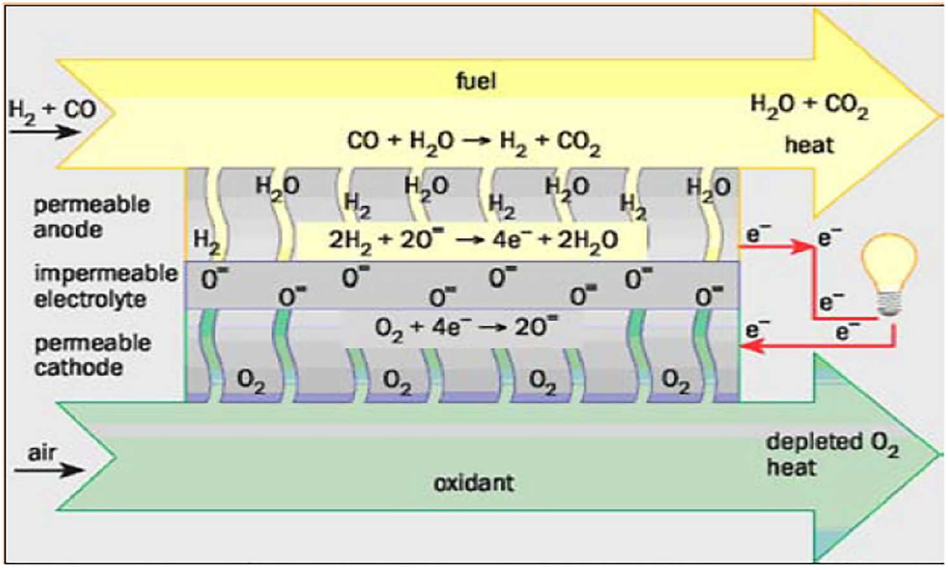

Fig. 1. Operating principle of a solid oxide fuel cell, adapted from Singhal [2].

operating lifespans, it is important to understand the environmental consequences of the proposed materials when presented in this context. To address these issues, a hybrid life cycle assessment is presented of three SOFC material structures (outlined in Section 3.3.1) to deduce their relative environmental impacts. This will provide valuable information to material researchers and SOFC developers regarding the environmental hotspots of the different material structures.

1.1. Contributions and novelty

Although the environmental impacts of the full life cycle of a product or service provides important information for society, it has been shown that conducting life cycle assessment (LCA), in the early stages of product development, is beneficial to avoid the generation of "green" assumptions about the materials under investigation [13,14]. Decreasing the operating temperature of SOFCs is paramount in their current development and this requires the use of novel material structures. Against this backdrop, the contributions and novelty of this paper are summarised as follows:

- This research is the first to compare the environmental impacts of the materials used in a commercial high temperature SOFC with new material structures under development (i.e. ESB and NBT) for intermediate temperature SOFCs. The results highlight the environmental implications of material substitution within the SOFC materials supply chain and quantify the impact of existing materials versus novel materials. This ensures that transitioning to novel materials does not outweigh the environmental benefits derived by reducing the operating temperature.
- It demonstrates the significance of taking into consideration, LCA, in decision support strategies when new materials are developed and considered in the substitution for other materials to ensure they are better in their environmental sustainability performance. Therefore, this research shows the need for LCA to become a 'standard routine' and an integral part of the toolbox of materials developer.
- Using the capabilities of LCA, this research shows that novel material combinations lead to a reduction in embodied materials and toxicological impact but higher electrical energy consumption during fabrication, in comparison to commercial SOFCs.
- Overall, this research contributes to the understanding of the implications of materials substitution, de-materialisation and waste mining on the materials market in which there are challenges due to scarcity, environmental impact and geo-political uncertainty of raw material supplies.

In the following section, a brief review of the literature on solid oxide fuel cells is provided.

2. Overview of published SOFC LCAs

To date, the main aim of published SOFC LCAs has been the identification of process and material environmental impacts, the possible effect of mitigation of these impacts and the comparison of energy sources [15]. For example, Strazza et al. [16] were able to show that for the ozone layer depletion, photochemical oxidation, acidification, eutrophication and non-renewable resources with energy content impact categories, the production of the fuel used in the SOFC led to the highest impact. For the global warming, the highest impact was from the use phase. Their results showed that the manufacturing of the SOFC is of relatively low impact.

Nease and Adams [17] presented a cradle-to-grave life cycle assessment of SOFCs utilized in large scale power plants which use the gasification of coal as fuel. Using the ReCiPe 2008 method, they compared their findings to the supercritical pulverised coal process and the integrated gasification combined cycle process. The pair have also compared bulk-scale SOFC power plants to the natural gas combined cycle using the same LCA method [18]. The functional unit chosen for these studies was 1 MWh of delivered electricity to allow a direct comparison of the results from the different processes [17,18].

Buchgeister [19] used the SOFC electricity generation from biomass as a case study to compare three LCA methodologies; eco-indicator 99, IMPACT 2002 and CML 2001. It was concluded that more than one methodology should be employed in order to produce a robust, quality result. In their review of SOFC LCAs, Mehmeti et al. [15] showed that the most frequently used environmental impact method was CML 2001 and the most common indicators were global warming potential, acidification potential, eutrophication potential and photochemical oxidation potential.

The use of liquefied propane gas to power microtubular SOFCs was investigated by Benveniste et al. [20]; a comparison of the environmental impacts of an auxiliary power unit and a conventional system were presented using LCA. The results of the study show that 54% of the overall global warming potential was caused by the production phase of the conventional system, but which could be minimised following changes to the fabrication process.

For a detailed review on SOFC, we refer readers to Stambouli and Traversa [21], where the arguments are detailed for the use of SOFCs as a solution to the pending limitation of fossil fuels due to their high efficiencies and flexibility on fuel use.

Although the current literature addresses important issues within the life cycle of SOFCs, none have been found to report the environmental impacts of materials substitution within their structures as industry moves to more novel materials. This is an important gap which this research seeks to fill.

3. Methodology

In this section, a detailed methodological framework for the comparative environmental profile evaluation of three SOFC material structures is presented. To reduce the operating temperatures of SOFCs, it is necessary to achieve the required properties using innovative, substituted materials. It has been shown by Ibn-Mohammed et al. [13] that life cycle assessment (LCA) plays a crucial role in product development in that one product may be assumed to be more "green" than another, but without a robust comparison of the environmental impact, this assumption should not be used in the decision making process.

3.1. Life cycle assessment

LCA methodologies are discussed widely in literature; the European standard ISO 14040:2006 defines the LCA process. Four phases are required to complete a robust LCA: definition of the goal and scope, an inventory analysis, an impact assessment and finally interpretation of the results [22–25]. The two leading techniques are process based LCA and environmental input-output (EIO) LCA [13,26–34]. The Supply Chain Environmental Assessment Tool- intelligence (SCEnAT*i*), developed by Koh et al. [35], integrates these two methodologies using a five step framework: supply chain mapping, carbon calculations, low carbon intervention, supply chain performance evaluation and informed decision making. This hybrid LCA approach assesses the complete supply chain, therefore providing a more robust result when compared to the process LCA methodology [36,37]. The decision support tool has been used successfully within a number of companies, leading to reductions in the environmental impacts of their supply chains [35,38]. The use of the hybrid LCA methodology through the SCEnAT*i* decision support system captures the supply chain inputs that may not be accounted for by a process LCA methodology [38].

3.2. Functional unit selection and system boundary

In the context of the current work, a hybrid LCA was conducted on three SOFC material structures; a commercial SOFC, an intermediate temperature SOFC utilising an erbia-stabilised bismuth oxide (ESB) electrolyte and a proposed intermediate temperature SOFC utilising a strontium doped sodium bismuth titanate (NBT) electrolyte. A functional unit of "kg of material required in the production of a 100 kW-

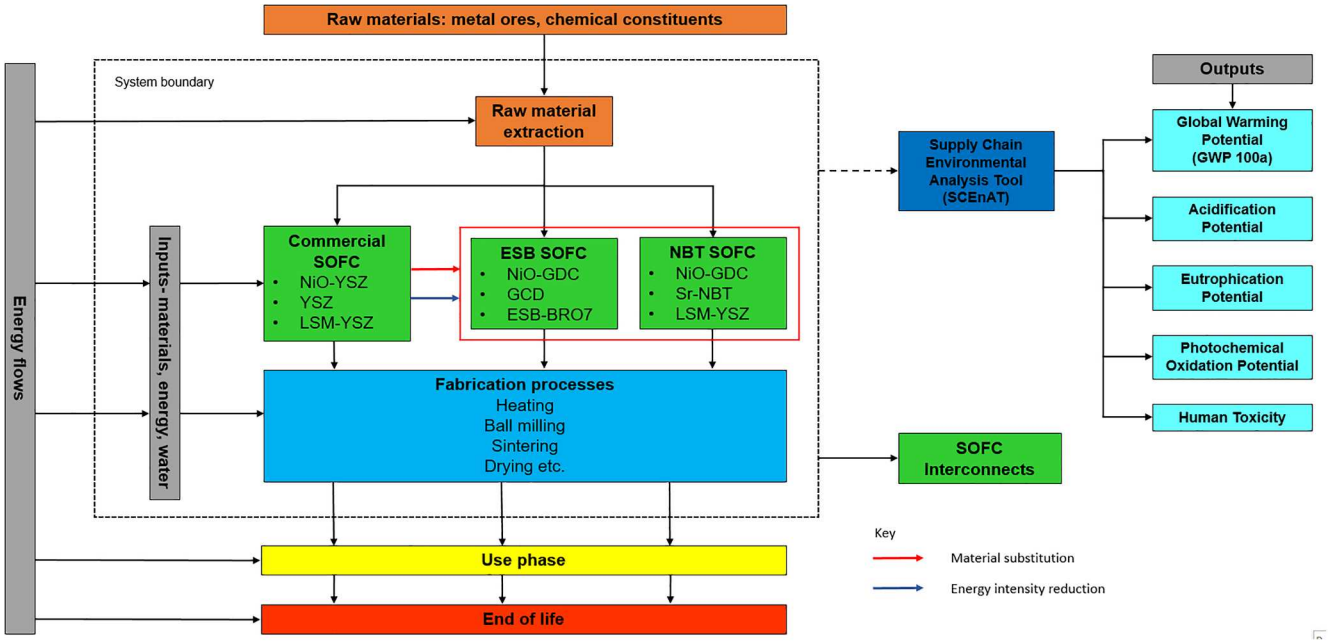

Fig. 2. The System boundary applied to the hybrid LCA of three SOFC material structures. N.B. the example fabrication processes listed are those shared by all three SOFC structures; see Section 3.3.1 for the specific manufacturing processes for each SOFC type.

class SOFC stack at installed capacity" was used, referred to from this point forward as "kg/100 kW energy generated"; all fuel energy values refer to the LHV. The manufacturing methods to produce each of the SOFC types are detailed in Section 3.3.1.

While LCA can take into account the whole life cycle of a product [39], the aim of this investigation is to understand the impact of the different material structures of the SOFCs, therefore the system boundary (shown in Fig. 2) includes raw material extraction and the SOFC manufacturing process; the use, end-of-life phases and interconnects are excluded. It is assumed that the lifespan of each material structure is similar and therefore it is not a factor in the analysis.

3.3. Data collection

While primary data is preferred for the completion of an LCA, where these are not available secondary sources can also be used [40]. In this study, the life cycle inventory was comprised of primary data from the laboratory and supplemented with secondary data from peer reviewed literature, and upstream emissions data from the Ecoinvent database [41]. Where material impact data were unobtainable, published guidelines on the use of stoichiometric reactions, chemical characteristics and functional parallels were used [13,42]. To achieve a deeper understanding of how the data for the LCA are generated, it is important to highlight the manufacturing processes for each of the SOFC materials architecture under consideration.

3.3.1. The SOFC manufacturing process

The manufacturing processes of each of the SOFCs are detailed in literature [43–46] and summarised in Section 3.3.1 a, b and c. Fig. 3 shows a schematic of the three SOFC structures that have been studied in this work: 3a) High temperature Commercial SOFC; 3b) Intermediate temperature NBT SOFC; 3c) Intermediate temperature ESB SOFC.

(a) The commercial SOFC manufacturing process

Anode production requires NiO, coarse YSZ and fine YSZ which are mixed at a ratio of 56:22:22 wt%. The resultant powder is ball milled in solvents for 24 h and then granulated using liquid granulation with a thermoset polymer. The final granules are then compacted and uniaxially pressed and then sintered in a reducing atmosphere for 3 h at 900 °C [43]. The YSZ electrolyte starts life as ZrO_2 (with 8 mol% Y_2O_3) powder which is ball milled with ethanol for 30 h. The mixture is then ultrasonically suspended in ethanol for 30 min in a mixture of 1 wt% ethylcellulose and 3 wt% polyvinyl butyral and finally sprayed on to the NiO/YSZ anode. The anode supported electrolyte is then sintered for 4 h at 1400 °C [44–46]. To complete the structure, LSM ($La_{0.7}Sr_{0.3}MnO_3$) and YSZ powders are mixed at a weight ratio of 6:4. This mixture is ground for 1 h with 6 wt% ethylcellulose and 94 wt% terpineol. The

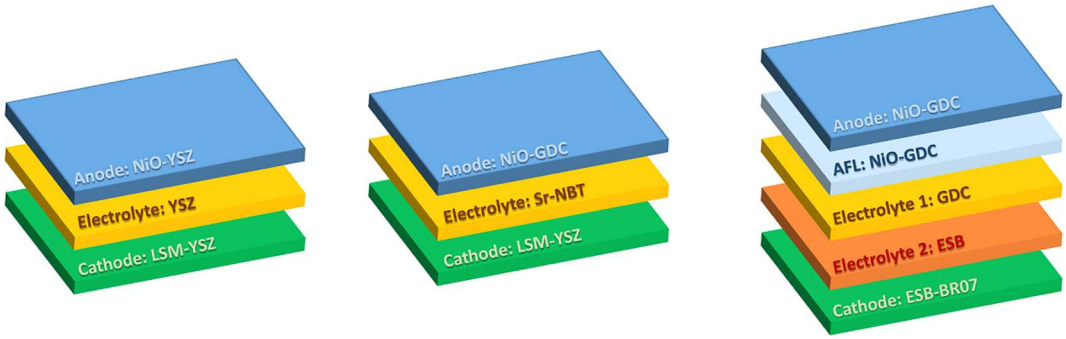

Fig. 3. Schematic of the three SOFC architectures studied in this article; from left to right: The Commercial HT-SOFC; the IT-SOFC with NBT electrolyte; the IT-SOFC with ESB electrolyte.

resulting paste is applied to the YSZ electrolyte by brush printing. The substrate is then sintered for 2 h at 1200 °C [46].

(b) The ESB SOFC manufacturing process

The anode support is produced by tapecasting NiO and $Ce_{0.9}Gd_{0.1}O_{1.95}$ powders at a 65:35 wt% ratio. The powders are weighed and ball milled with a dispersant (Solsperse, toluene and ethyl alcohol mixture) for 24 h. Di-n butyl phthalate (DBP), polyethylene glycol (PEG) and polyvinyl butral (PVB) are added to the suspension which is ball milled for a further 24 h. De-airing then takes place in a vacuum chamber, the slurry must be stirred continuously to prevent solidification. The slurry is then tapecast, dried for 2 h at 100 °C, shaped into discs and finally sintered at 900 °C for 2 h [47]. The anode functional layer (AFL) is also produced using GDC powder, the solution is prepared with ethanol and sprayed on to the NiO-GDC anode; presintering then takes place at 900 °C for 1 h [47,48]. GDC powder is then ball milled for 24 h with Solsperse in ethanol, Di-n butyl phthalate (DBP) and polyvinyl butral (PVB) are then added prior to a further 24 h of ball milling. The slurry is then spray coated on to the NiO-GDC anode (and AFL). The Electrolyte-AFL-Anode substrate is heat-treated in a vacuum oven for 5 h at 120 °C and then sintered at 1450 °C for 4 h [47,48].

The ESB electrolyte is produced using Er_2O_3 and Bi_2O_3 powders which are weighed, ball milled in ethanol using yttria-stabilized zirconia (YSZ) media for 24 h, dried on a hot plate with stirring and then calcined at 800 °C for 15 h. The ESB green pellets are produced by uniaxially pressing (at around 10Kpsi); firing at 890 °C for 4 h [49,50]. Pulsed Laser Deposition (PLD) is used to deposit the ESB electrolyte on to the GDC electrolyte. The substrate (anode and AFL) is heated to 630 °C.

The BRO7-ESB cathode is manufactured using $Bi_2Ru_2O_7$ and ESB. Stoichiometric amounts of Bi_2O_3 and $RuO_2{\cdot}XH_2O$ are combined to produce BRO7. The powder is ball milled in ethanol for 24 h with grinding media of YSZ, dried on a hotplate whilst being stirred and then calcined at 900 °C for 10 h [50]. The resultant powder is then crushed and sieved [50]. The ESB (production method described above) and BRO7 powders are then mixed with isopropanol and ultrasonicated. Paint brushing is then used to apply the slurry to the electrolyte. The substrate is then dried for 1 h at room temperature, dried at 120 °C for 1 h and fired at 800 °C for 2 h [50].

(c) The NBT SOFC manufacturing process

The NBT SOFC is currently in the conceptual phase and to date the electrolyte alone has been manufactured. It is therefore assumed that the electrolyte will be used in conjunction with a NiO-GDC anode and a LSM-YSZ cathode as these are the most commonly used materials in each case. In this case, the anode (NiO-GDC) is produced in the same method outlined in Section 3.3.1b. The Sr-doped NBT electrolyte is produced through solid state synthesis using Na_2CO_3, Bi_2O_3, $SrCO_3$ and TiO_2; before weighing, each constituent is dried at 300 °C (Na_2CO_3, Bi_2O_3), 180 °C ($SrCO_3$) and 800 °C (TiO_2), respectively. The mixture of powders is ball milled for 6 h, dried (12 h at 80 °C), sieved and calcined for 2 h at 800 °C. A second calcination takes place at 850 °C for 2 h, followed by ball milling for 6 h. Finally, pellets are sintered at 1150 °C for 2 h in air [51]. Cathode materials for NBT-based electrolyte are still under investigation. In this study, the LSM-YSZ cathode of the commercial SOFC is used as a representative example. The final substrate is dried for 1 h at room temperature, dried at 120 °C for 1 h and then fired at 850 °C for 2 h.

3.3.2. Building a functional SOFC

Section 3.3.1 a, b and c describe the production of one cell of a SOFC, in reality, cells are stacked to form modules in order for them to achieve the required power output. Wachsman et al. [6] report the dimensions of one SOFC cell as 10 cm × 10 cm × 0.2 cm (width x length x height). The heights of each component within the cell structure are reported as 800 μm (anode), 1 μm (anode functional layer), 10 μm (GDC electrolyte), 4 μm (ESB electrolyte) and 49 μm (cathode), the remaining height represents the interconnect [47,48,52]. One module is required to produce 100 kW; one module contains 10 stacks, 1 stack contains 50 cells, therefore 1 module contains 500 cells. The calculated kg required for one cell were then scaled appropriately. As the NBT structure is still under development, in order to complete the data acquisition for the process LCA, it was assumed that the NBT structure was of the same size and output as the ESB structure. Using this information, the weights of the NBT structure were acquired.

3.3.3. Life cycle impact categories

The environmental impacts analysed in this case were taken from the Ecoinvent database (version 3.2 2105) and used as the method of comparison between the three SOFC structures. The impacts chosen were those highlighted by Mehmeti et al. [15] as the most frequently used in SOFC LCA analysis and taken from the CLM 2001 database; global warming potential (GWP) 100a, acidification potential (AP) generic, eutrophication potential (EP) generic, freshwater aquatic ecotoxicity potential (FAETP) 100a, freshwater sediment ecotoxicity potential (FSETP) 100a, marine aquatic ecotoxicity potential (MAETP) 100a, marine sediment ecotoxicity potential (MSETP) 100a, human toxicity potential (HTP) 100a and land use. The cumulative energy demand (i.e. materials embodied energy) was also compared and is the primary energy relating to the extraction of embodied energy of natural resources that has not been transformed into any usable energy such as electricity or gas. Examples include fossil fuels, solar, nuclear, geothermal and wind energy [13,53], therefore, the cumulative energy demand is equal to the sum of the aforementioned energy sources. In line with the conclusions made by Buchgeister [19], the ReCiPe 2008 data set are also analysed to support the CML2001 impacts and allow for further assessment.

The Ecoinvent dataset for the “market for electricity, low voltage [kWh]” represented the electricity used in this investigation. This dataset reveals the feeding of electricity into the network, including all upstream activities, i.e. generation (reference product: electricity, low voltage [kWh]). The thermal energy consumption was shown using “heat and power co-generation, natural gas, combined cycle power plant, 400 MW electrical [MJ]; representing the production of high voltage electricity and heat in a combined cycle natural gas power plant (reference product: heat, district or industrial, natural gas [MJ]). Both datasets relate to generation in Great Britain.

Component level analysis of different environmental impact categories were normalised to identify the significance of each element of the SOFCs. The total primary energy demand within the system boundary was determined.

The SCEnAT*i* decision support tool was utilised to enable the indirect impacts of manufacturing the SOFC structures to be accounted for. In this case the following ‘missing inputs’ were applied to the system boundary of the chosen supply chain: freight transport by road, telecommunications, computer services and related activities, research and development, collection of waste.

3.3.4. Life cycle inventories

The breakdown of the electrical and thermal energy consumptions for the production of each of the material structures studies are shown in Tables 1–6. It is important to note that those laboratory processes conducted manually and which do not require an energy input, have been excluded from Tables 1–6. Table 7 outlines the equivalent energy demand for both electricity and gas in MJ-eq based on generic data from Ecoinvent. The SOFC structure life cycle inventories relating to each of the SOFC structures are outlined in the Appendix in Tables A1–A3.

As highlighted in Section 3.3.3, the materials embedded energy, which is expressed in MJ-eq, is the sum of the untransformed energy sources including fossil fuels, solar, nuclear, geothermal and wind energy as outlined in Table 7. For example, the energy consumption of the calcination of ESB (shown in Table 5) is equal to 31.05 kWh but, as shown in Table 7, 1 kWh of energy is equivalent to 11.84 MJ-eq.

Table 1
Electrical energy consumption for the production the commercial SOFC structure.

Process flow	Equipment power rating (W)	Time (s)	Electrical energy (kWh)
Ni heating	2070	21,600	12.42
Ball mill NiO-YSZ	50	86,400	1.20
Sintering of NiO-YSZ	2070	10,800	6.21
Ball mill YSZ	50	108,000	1.50
Ultrasonic suspension of YSZ	250	1800	0.13
Sintering YSZ	2070	14,400	8.28
Sintering of LSM-YSZ	2070	7200	4.14
Total			33.88

Accordingly, the primary energy demand for the calcination of ESB is 372.96 MJ-eq. This is necessary to allow for the three energy types to be compared using the same units.

4. Results and discussion

The results shown in Figs. 4–11 graphically evaluate the impact of each of the three SOFC structures which have been investigated; Commercial, NBT and ESB. The materials which constitute each component within the structure, i.e. anode, cathode etc. have been amalgamated to demonstrate the environmental impact of the component and to reduce the complexity of the figures. Where a substantial impact is caused by one of the materials used within the component, this is discussed in further detail.

4.1. Comparison of the environmental profiles of the SOFC structures

Fig. 4a shows a total primary energy demand for the production of a commercial SOFC as 48,368 MJ-eq/100 kW; this is dominated by the material embedded energy which accounts for almost 97% of the total. In comparison, the total primary energy demand of the NBT SOFC is 19,481 MJ-eq/100 kW; in this case, the percentage contribution of the electrical energy demand is 44%. Similarly, the electrical energy consumption for the production of the ESB material structure is 38% with a total primary energy demand of 24,064 MJ-eq/100 kW. In all three cases, the thermal energy consumption accounts for less than 1% of the total.

As discussed in Section 3.3.1, the manufacturing process of the intermediate temperature SOFC structures are more complex than that of the commercial SOFC, leading to an increased electrical energy requirement. For example, the NiO-GDC anodes of the IT-SOFC structures require an additional de-airing and tapecasting step, which the HT-SOFC structure does not. Furthermore, the IT-SOFC NBT electrolyte and IT-SOFC ESB electrolyte require a calcination step, absent from the manufacturing process of the HT-SOFC.

Despite this, the overall primary energy use of the intermediate structures is lower due to a reduced material embedded energy in these structures. This reduction can be attributed to the change from a NiO-YSZ anode to a NiO-GDC anode and a reducing in the amount of material required to achieve the same power output (discussed above), leading to a saving of 35,318.3 MJ-eq/kg. While the overall percentage contribution of YSZ is higher than GDC, the intermediate anodes require a much smaller amount of GDC in the manufacturing process and therefore the overall impact is lowered.

There is larger difference in the material embedded energy of the HT-SOFCs when compared with the LT-SOFCs due to the amount of material required to achieve the functional unit of kg/100 kW of energy

Table 3
Electrical energy consumption for the production the NBT SOFC structure.

Process flow	Equipment power rating (W)	Time (s)	Electrical energy (kWh)
Ni Heating	2070	21,600	12.42
Weigh NiO	230	60	0.004
Weigh GDC	230	60	0.004
Ball mill NiO-GDC	50	172,800	2.40
De-airing with continuous stirring of NiO-GDC	1020	86,400	24.48
Tapecasting of NiO-GDC	4600	1800	2.30
Dry NiO-GDC	2070	7200	4.14
Sinter NiO-GDC	2070	7200	4.14
Dry Na_2CO_3	2070	43,200	24.84
Dry Bi_2O_3	2070	43,200	24.84
Dry $SrCO_3$	2070	43,200	24.84
Dry TiO_2	2070	43,200	24.84
Weigh Na_2CO_3	230	60	0.004
Weigh Bi_2O_3	230	60	0.004
Weigh $SrCO_3$	230	60	0.004
Weigh TiO_2	230	60	0.004
Ball mill Sr-NBT	50	21,600	0.30
Dry Sr-NBT	2070	43,200	24.84
Calcine Sr-NBT	2070	7200	4.14
	2070	7200	4.14
Ball mill Sr-NBT	50	21,600	0.30
Sinter Sr-NBT	2070	7200	4.14
Sinter LSM-YSZ	2070	7200	4.14
Dry	2070	3600	2.07
Dry	2070	3600	2.07
Sinter	2070	7200	4.14
Total			199.54

Table 4
Thermal energy consumption for the production the commercial NBT structure.

Process flow	Temp' (K)	SHC* (J/mol K)	Mass (kg)	Mol	Thermal energy (MJ)
Ni Heating	673	26.10	10.94	186.42	3.27
Dry NiO-GDC	373	52.25	16.84	67.99	1.33
Sinter NiO-GDC	1173	52.25	16.84	67.99	4.17
Dry Na_2CO_3	573	112.30	0.06	0.58	0.04
Dry Bi_2O_3	573	113.50	0.25	0.55	0.04
Dry $SrCO_3$	453	81.40	0.01	0.05	0.002
Dry TiO_2	1073	55.00	0.19	2.31	0.14
Dry Sr-NBT	353	101.40	0.51	2.00	0.07
Calcine Sr-NBT	1073	101.40	0.51	2.00	0.22
	1123	101.40	0.51	2.00	0.23
Sinter Sr-NBT	1423	101.40	0.51	2.00	0.29
Sinter LSM-YSZ	1473	78.75	5.25	16.10	1.87
Dry	298	63.04	27.61	320.72	6.03
Dry	393	63.04	27.61	320.72	7.95
Sinter	1123	63.04	27.61	320.72	22.71
Total					48.33

Table 2
Thermal energy consumption for the production the commercial SOFC structure. *Specific heat capacity.

Process flow	Temp' (K)	SHC* (J/mol K)	Mass (kg)	Mol	Thermal energy (MJ)
Ni heating	673	26.10	68.88	1173.42	20.61
Sintering of NiO-YSZ	1173	51.23	123.00	1646.59	98.94
Sintering YSZ	1673	59.90	2.14	17.40	1.74
Sintering of LSM-YSZ	1473	78.75	5.25	16.10	1.87
Total					123.17

Table 5
Electrical energy consumption for the production the commercial ESB structure.

Process flow	Equipment power rating (W)	Time (s)	Electrical energy (kWh)
Ni Heating	2070	21,600	12.42
Weigh NiO	230	60	0.004
Weigh GDC	230	60	0.004
Ball mill NiO-GDC	50	172,800	2.40
De-airing with continuous stirring of NiO-GDC	1020	86,400	24.48
Tapecasting of NiO-GDC	4600	1800	2.30
Dry NiO-GDC	2070	7200	4.14
Sinter NiO-GDC	2070	7200	4.14
Presinter GDC	2070	3600	2.07
Ball mill GDC	50	172,800	2.40
Heat treat GDC	2070	18,000	10.35
Sinter GDC	2070	14,400	8.28
Weigh Er_2O_3	230	60	0.004
Weigh Bi_2O_3	230	60	0.004
Ball mill ESB	50	86,400	1.20
Dry ESB on hot plate while stirring	1020	86,400	24.48
Calcine ESB	2070	54,000	31.05
Sinter ESB	2070	14,400	8.28
PLD of ESB	30,000	2700	22.50
Ball mill BRO7-ESB	50	86,400	1.20
Dry BRO7-ESB on hot plate while stirring	1020	86,400	24.48
Calcine BRO7-ESB	2070	36,000	20.70
Ultrasonication of BRO7-ESB	250	1800	0.13
Dry BRO7-ESB	2070	3600	2.07
	2070	3600	2.07
Sinter	2070	7200	4.14
Total			215.29

Table 6
Thermal energy consumption for the production the commercial ESB structure.

Process flow	Temp' (K)	SHC* (J/mol K)	Mass (kg)	Mol	Thermal energy (MJ)
Ni Heating	673	26.10	10.94	186.42	3.27
Dry NiO-GDC	373	52.25	16.84	67.99	1.33
Sinter NiO-GDC	1173	52.25	16.84	67.99	4.17
Presinter GDC	1173	66.34	0.03	0.20	0.02
Heat treat GDC	393	66.34	0.34	1.96	0.05
Sinter GDC	1723	66.34	0.34	1.96	0.22
Dry ESB on hot plate while stirring	373	112.65	0.17	0.38	0.02
Calcine ESB	1073	112.65	0.17	0.38	0.05
Sinter ESB	1163	112.65	0.17	0.38	0.05
PLD of ESB	903	112.65	0.17	0.38	0.04
Dry BRO7-ESB on hot plate while stirring	373	98.49	12.82	20.72	0.76
Calcine BRO7-ESB	1173	98.49	12.82	20.72	2.39
Dry BRO7-ESB	298	98.49	12.82	20.72	0.61
	393	98.49	12.82	20.72	0.80
Sinter	1073	98.49	12.82	20.72	2.19
Total					15.96

generated. 123 kg of Ni-YSZ is required for the anode of the HT-SOFC alone, in comparison to only 17 kg of NiO-GDC for both of the IT-SOFC architecture anodes. These amounts were calculated based on those provided in published literature, in line with Section 3.3.1.

Fig. 4b compares the toxicological footprints of each material structure with respect to the HTP, FAETP, FSETP, MAETP and MSETP, all measured in kg 1,4-DCB-eq. Of the five indicators studied, the MAETP and MSETP impacts have the highest result over each of the three SOFC structures. It is the use of NiO in the anodes of the commercial HT-SOFC and the NBT IT-SOFC that causes, over 97% and 88% respectively, the overall impact of the component for these five

Table 7
Equivalent energy demand for both electricity and gas in MJ-eq based on generic data from Ecoinvent.

Cumulative energy demand (MJ-eq)	Electricity (electrical energy- kWh)	Gas (thermal energy-MJ)
Biomass	0.51	0.0002
Fossil	7.71	0.44
Geothermal	0.00	0.000
Nuclear	3.25	0.001
Primary forest	0.001	1.34E-06
Solar	0.02	1.30E-07
Water	0.10	0.001
Wind	0.24	5.40E-05
Total	11.84	0.44

toxicological indicators.

Although the NiO-GDC anode of the ESB IT-SOFC leads to almost 75% of the HTP impact, it is the use of ruthenium oxide in the cathode that results in the highest impact over the four remaining toxicological indicators. Ruthenium is a platinum group metal (PGM), the use of $RuO_2{\cdot}XH_2O$ in the ESB cathode structure may cause a high toxicological result because certain compounds of PGMs have been found to have carcinogenic and mutagenic effects [54].

Fig. 4c gives a comparison of the ReCiPe Endpoint (E, A) 2008 environmental impact category; the result provided by this indicator mirrors the results of those given by the CML2001 indicator in Fig. 4b. Although the methodologies differ and therefore the two results cannot be directly compared, it is important to show the results across a range of methodologies [55].

The IO upstream GHG data was inputted into the SCEnAT*i* decision support tool. A comparison of the results for each structure is shown in Fig. 4d. In each case, the highest proportion of the impact can be attributed to the 'transport and communication' sector, followed by 'mining' and 'utilities'. Again, the upstream GHG data for the commercial SOFC architecture is higher than that of the NBT and ESB structures because of the higher amount of material required for the production of the commercial SOFC, leading to a higher impact on the supply chain. As these impacts would usually be excluded from a process LCA, their inclusion in this analysis gives a more accurate life cycle impact result [26].

4.1.1. A closer look at material use vs. electrical energy consumption impacts

State of the art SOFC stacks have been reported to function for no more than 2–3 years because of issues such as mechanical stresses and catalyst poisoning. To determine the energy payback period (EPP) for each of the material structures concerned, a knowledge of the energy outputs of each type of SOFC is required. Given that ESB and NBT SOFCs are still under development, it is difficult to estimate their electrical energy outputs and consequently their EPP cannot be calculated at this time. However, it is important to shed more light on the interplay between embodied materials impact and impact due to electrical energy consumed during fabrication. As shown in Table 8, if the energy outputs were known, it is immediately clear that NBT SOFC will yield the fastest energy payback period followed by ESB SOFC. However, as shown in Fig. 5, the split between materials and energy consumption impacts is 86%: 14% and 81%: 19% for ESB and NBT SOFCs respectively compared to 99%:1% for commercial SOFCs.

While the electrical energy requirements of the novel SOFC materials structures increases in comparison to the commercial SOFCs, we argue that achieving lower materials impact has greater influence than energy consumption. It is easier to specify intervention options for energy reduction which are readily available compared to impact which requires optimisation of properties for the reduction in usage or through intelligent specifications of materials with lower embedded impact. In an industrial setting, mass production of the SOFC stacks

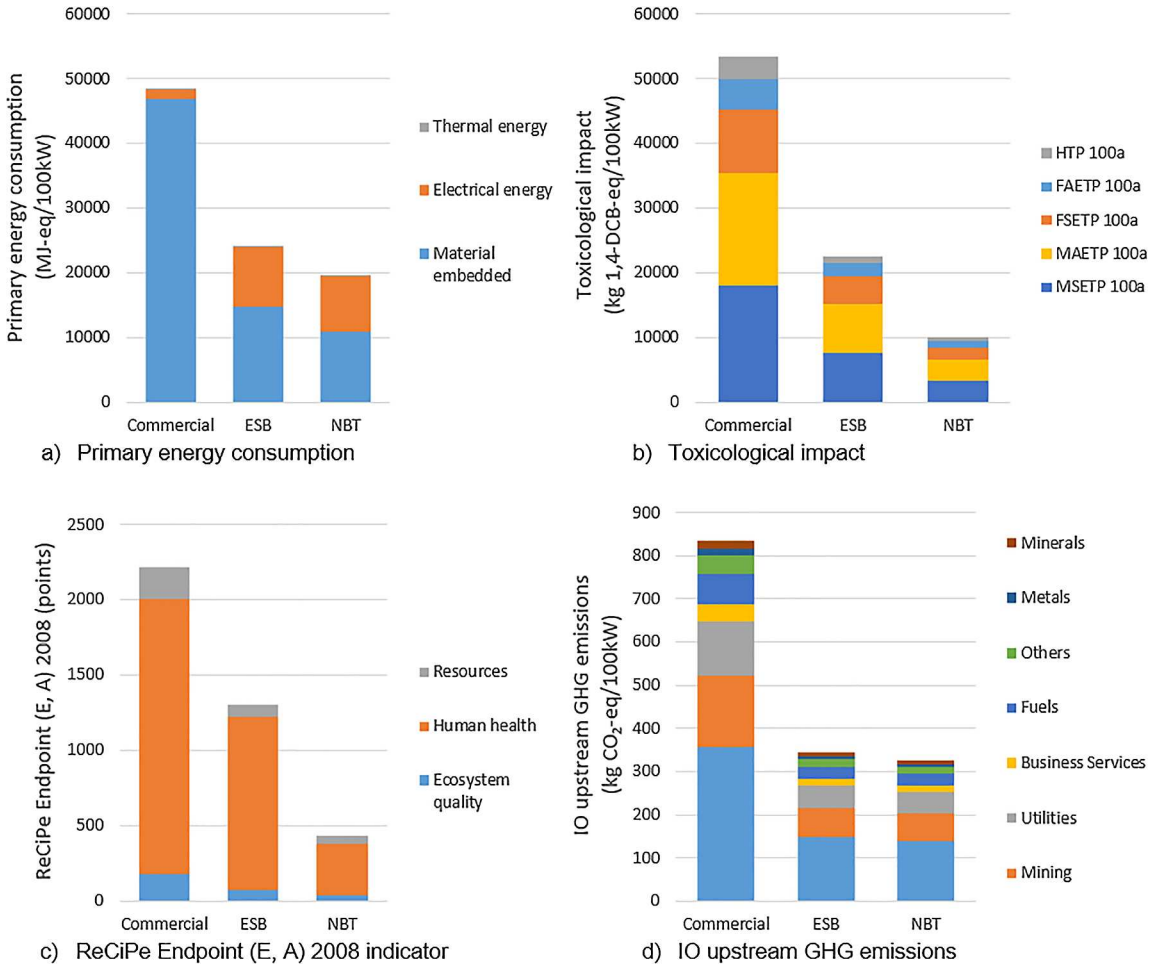

Fig. 4. The comparison of the commercial, NBT and ESB SOFC material structures for (a) primary energy demand, (b) toxicological footprint, (c) ReCiPe Endpoint (E, A) 2008 and (d) IO upstream greenhouse gas (GHG) emissions.

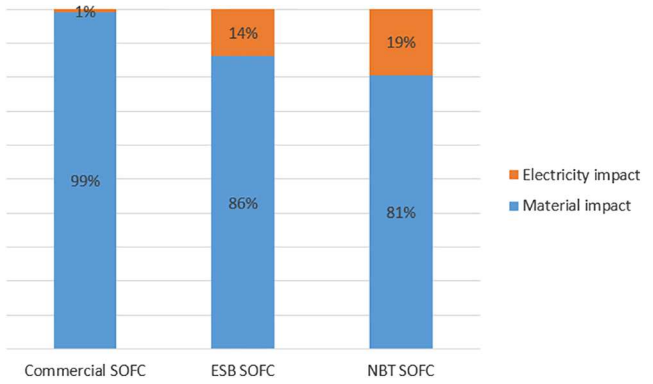

Fig. 5. Percentage contribution of the electrical and material energy impacts for the GWP 100a indicator.

would be employed, thereby reducing the electrical and thermal loads by more efficient processing methodologies [52]. New techniques such as cold sintering are also being developed to reduce energy consumption during the densification of ceramics [56] and optimised rotational speed and the improved grinding capacity in industry may be used to reduce the electrical energy attributed to ball milling on the laboratory scale [57]. Moreover, if in the future, the grid is de-carbonised and the emissions intensity of electricity is greatly reduced, the overall electrical energy consumption will lessen leaving the challenge to determine how impact from materials may be minimised. Essentially, despite the higher energy consumption of ESB and NBT SOFCs, the work reported here still constitutes a significant reduction in impact due to materials utilisation in the development of SOFCs.

4.2. Primary energy consumption of commercial, ESB and NBT SOFCs

This section provides an evaluation of the material embedded distributions, thermal and electrical energy distributions (Figs. 6–8) for each of the SOFC structures that have been studied (commercial, NBT and ESB, respectively).

The material embedded energy contributions for each material structure are broken down further in Figs. 6–8a. For both the Commercial and NBT structures (Figs. 6–8a), the anode composite structures lead to the highest impact. Deeper inspection of the analysis shows that for the commercial SOFC, YSZ contribution is 58% while the NiO contribution is 25%. Similarly, 68% of the NBT SOFC anode material embedded energy is caused by the use of Gd-doped CeO_2 (GDC). Figs. 6–8a shows that the NiO-GDC anode of the ESB SOFC contributes to 53% of the material embedded energy while just under 47% is caused by the cathode. With the cathode however, the impact is caused by the use of ESB.

While the thermal energies of each of the material structures are negligible in comparison to the material embedded and electrical energies, in each of the three cases shown in Figs. 6–8b, the highest impact comes from the sintering process. “Others” in Figs. 6–8b refers to processes below 1% such as pre-sintering and pulsed laser deposition. Figs. 6–8c shows that the highest electrical impact of the commercial SOFC material structure is also from sintering, whereas Figs. 6–8c show that drying has the highest electrical energy contribution in the

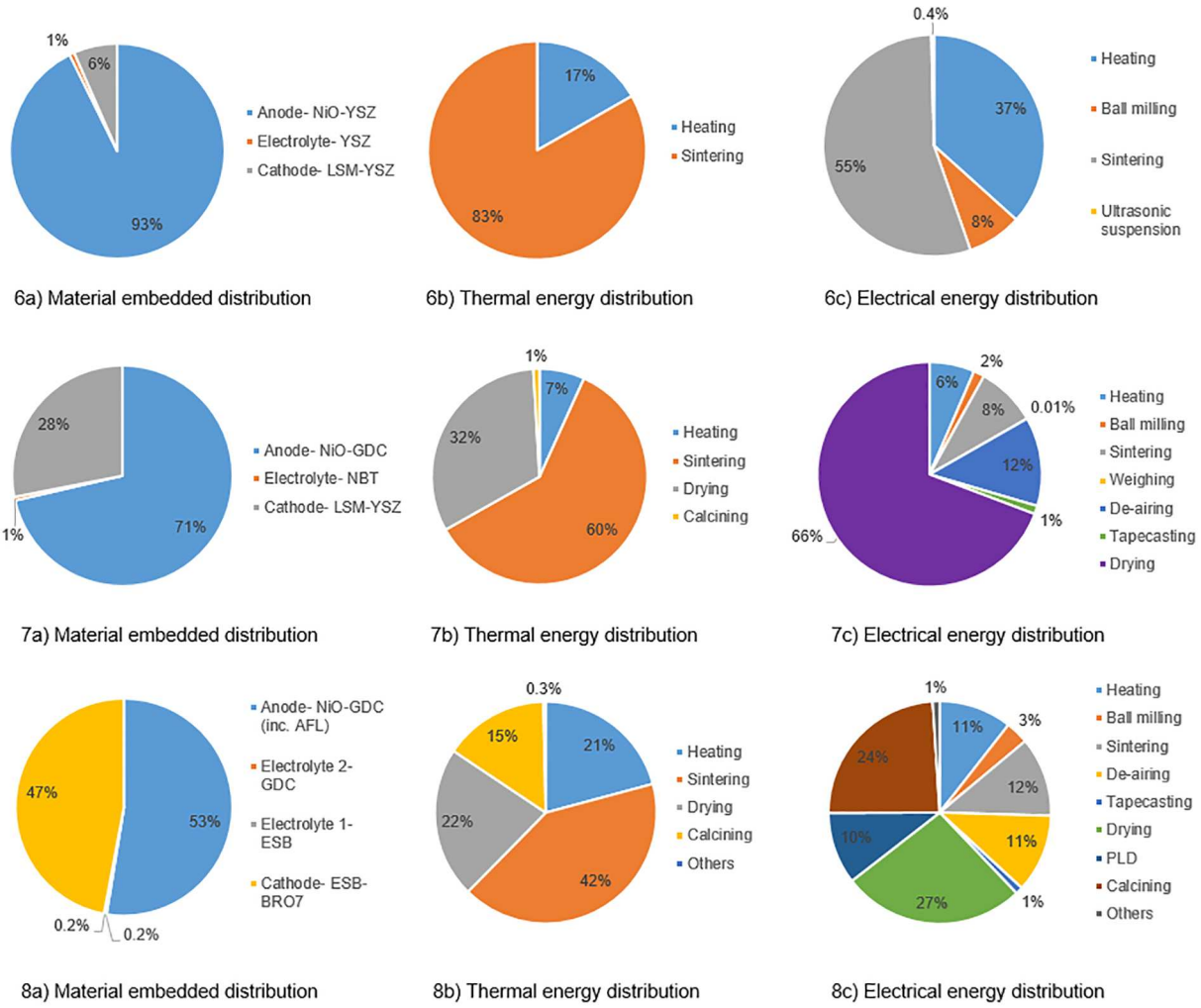

Figs. 6–8. The percentage contribution of each process step in relation to the primary energy consumption shown in Fig. 4a.

intermediate temperature SOFCs. “Others” in Figs. 6–8c refers to those processes below 1%, namely: weighing, pre-sintering and ultrasonication.

It is clear to see in Figs. 6–8b and c, that the manufacturing processes becomes more complicated as the operating temperature decreases. Consequently, the electrical energy requirements increase. Should either of these structures be commercialised, it is likely that the thermal and electrical energy demands will be reduced due to the use of more energy efficient machinery and a batch manufacturing process with a higher output [58]. Additionally, it has been shown by Ibn-Mohammed et al. [13] that the use of sintering aids and low temperature manufacturing technology can further optimise the sintering process and consequently reduce the thermal and electrical energy requirements.

4.3. Component level analysis of each SOFC structures

The NiO-YSZ anode in the commercial SOFC structure causes the highest environmental impact, shown in Fig. 9 (the axis of which ranges from 80 to 100% to clearly show the impact of each element in the structure). Within the anode, the use of NiO has the highest contribution to the AP (89%), EP (78%), FAETP 100a (86%), HTP 100a (81%), MAETP 100a (88%), FSETP 100a (86%) and MSETP 100a (87%). While the environmental impact of nickel mining has decreased, historically it has caused heavy metal soil contamination, a reduction in biodiversity and acid rain [59]. With regards to human toxicology, nickel inhalation has been linked to lung and nose cancer [60]. The use of YSZ in the component contributes to 55% of the GWP 100a of the commercial SOFC anode, the cumulative energy demand of this material contributes to 58% of the overall anode total and the land use category, which expresses land damage (e.g. occupation) in square meter of land per year, is 61%.

It is the use of ZrO_2 in YSZ that leads to the highest impact across the GWP (56%), AP (44%), EP (59%), FAETP (60%), MAETP (61%), CED (35%), FSETP (61%) and MSETP (61%) indicators. ZrO_2 is produced by the calcination of zirconium hydroxide which is synthesised during the zirconium-hafnium separation process [61]. Zirconium mining leads to high energy use for the dredging activities and diesel for machinery such as trucks and excavators (affecting the GWP and CED impact). Mineral separation leads to the release of heavy metals which contributes to the ecotoxicity impacts (FAETP, MAETP, FSETP and MSETP) of the material. Additionally, the release of greenhouse gases directly affects the AP impact of the material [61,62].

The overall impact of the NBT SOFC is also mainly affected by the impact of the NiO-GDC anode; GWP 100a (73%), AP (95%), EP (88%), FAETP 100a (92%), HTP 100a (88%), MAETP 100a (92%), CED (71%), FSETP 100a (92%), MSETP 100a (92%) and Land use (61%); this is shown in Fig. 10. While the majority of this impact can be attributed to the NiO component of the anode, the cumulative energy demand (68%), land use (46%) and GWP 100a (58%) are caused by the use of GDC. In turn, the cerium component of GDC, causes this.

In comparison to this, the ESB SOFC environmental impact is mainly shared across the impacts of the anode (NiO-GDC) and the cathode (ESB-BRO7); Fig. 11. While the impacts of the NiO-GDC anode are mentioned in the previous paragraph, the majority of the cathode impacts are affected by the use of $RuO_2{\cdot}XH_2O$. Ruthenia is found in very

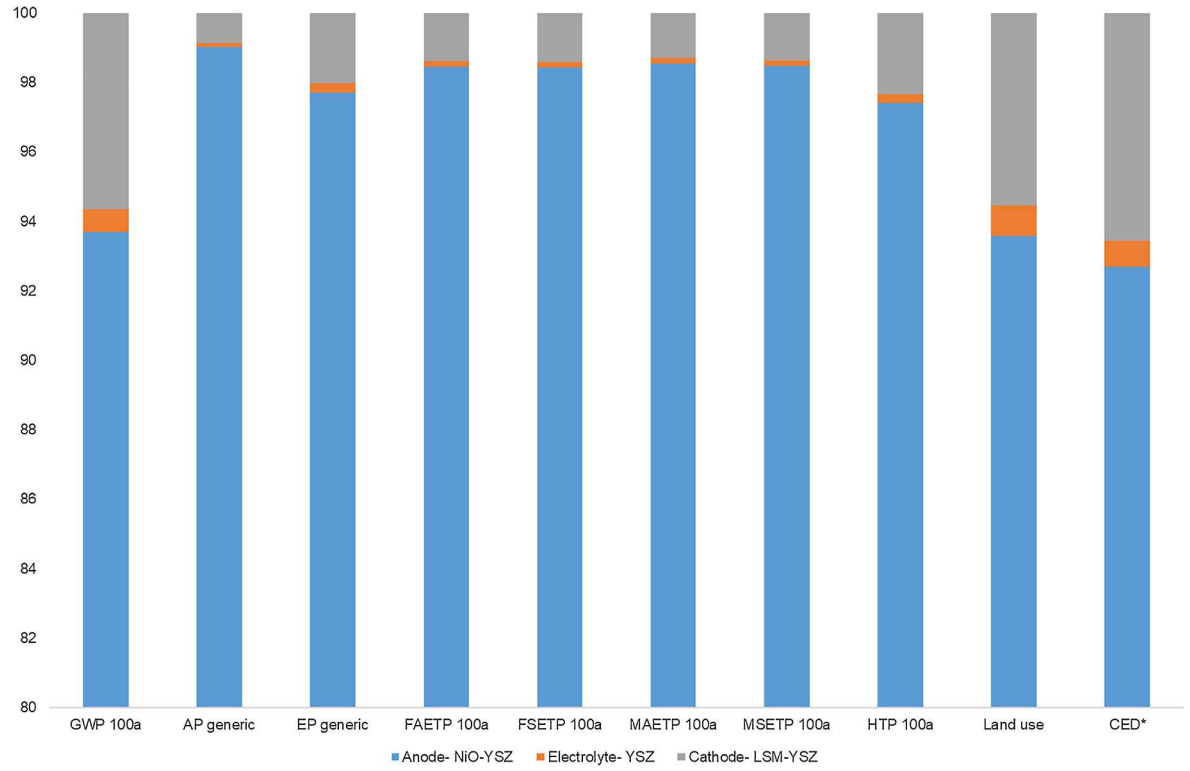

Fig. 9. The percentage contribution of each commercial SOFC component for the environmental impacts investigated in this study. The y axis is shown from 80% to 100% to show the impact contribution from all three components.

small quantities in ores in combination with other platinum metals; it is difficult to separate from those ores [63,64]. Mining of platinum group metals is an energy and labour intensive process that can take up to six months due to its complexity, leading to a high environmental impact due to high electricity consumption [65].

An overall comparison of each environmental impact category shows that the NBT materials lead to the lowest of the three material structures in all of the investigated cases. With this in mind, overall, the NBT intermediate temperature SOFC provides the lowest environmental impact of the three structures that were investigated in this study.

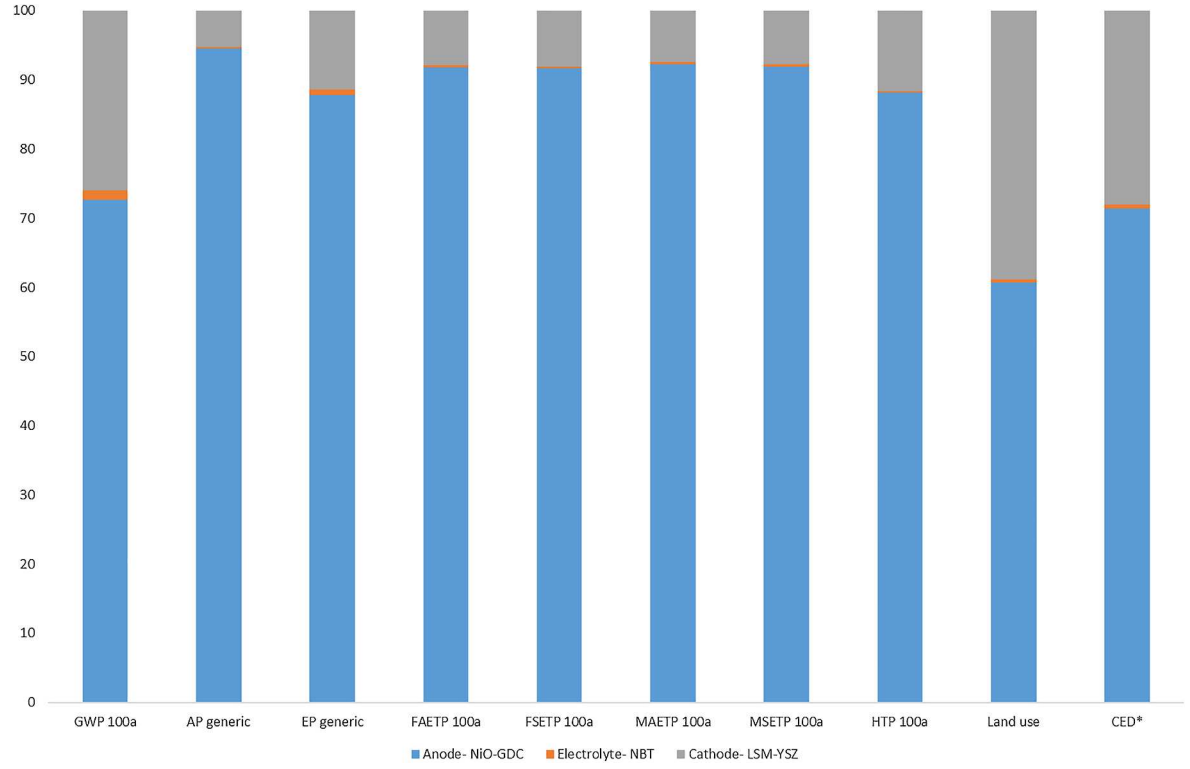

Fig. 10. The percentage contribution of each NBT intermediate temperature SOFC component for the environmental impacts investigated in this study.

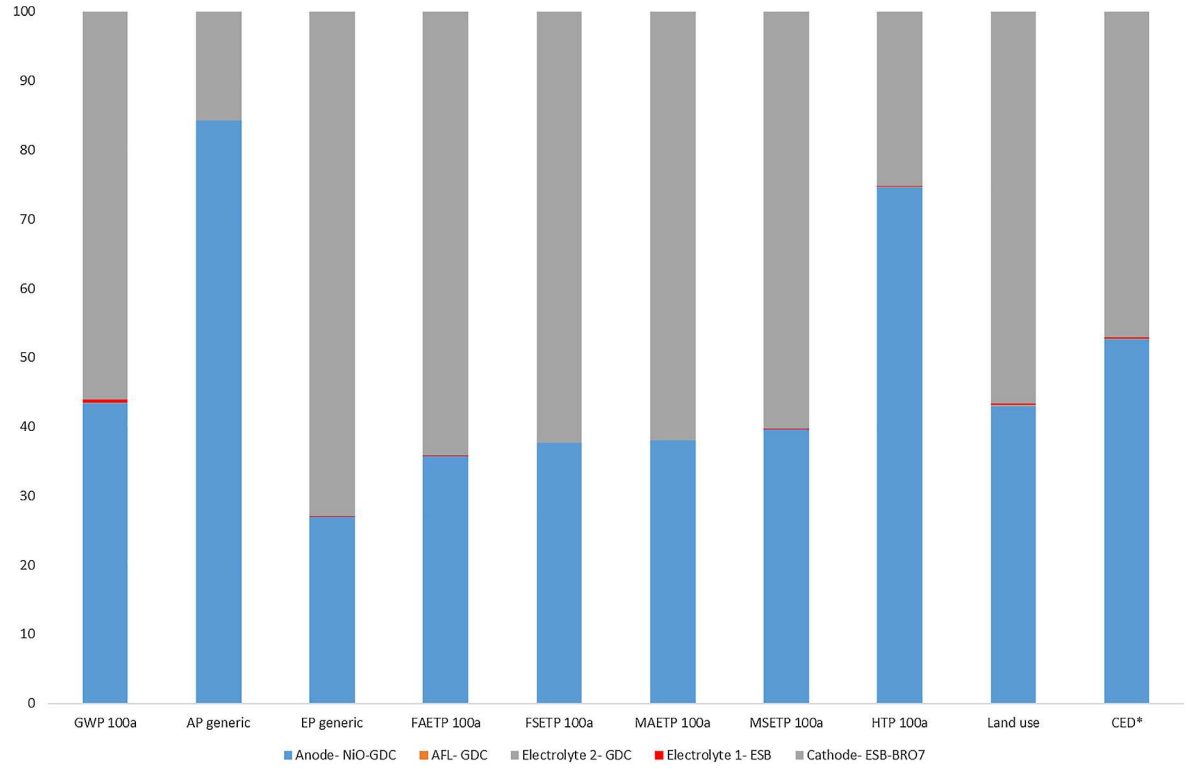

Fig. 11. The percentage contribution of each ESB intermediate temperature SOFC component for the environmental impacts investigated in this study.

Table 8
Materials vs electrical energy impact of each of the three SOFC structures.

Impact category	Commercial SOFC	ESB SOFC	NBT SOFC
Material impact ($kgCO_2$-eq)	2382.64	866.99	517.59
Electricity impact ($kgCO_2$-eq)	22.00	139.84	124.23
Total impact ($kgCO_2$-eq)	2404.64	1006.83	641.82

What each of these structures has in common is their use of rare earth elements (REEs) which are mined as rare earth oxides (REOs). REOs have been classified as critical by the European Union [66] and while they are not rare in abundance, they are difficult to mine in often unfeasibly economic concentrations [67,68]. Their production process leads to mining wastes, chemical pollution, hazardous wastewater discharge, greenhouse gas emissions and resource depletion (among other impacts) [69]. Throughout the material structures, it is this factor (along with the use of nickel) that has the highest overall impact.

4.4. Limitations of the presented work

The bill of materials for the commercial and ESB material structures was acquired from literature, the NBT structure was taken from literature and developed further by expert knowledge of the functional requirements. A lack of primary data is the main limitation to the output of the study. Further development of the NBT components will allow for a more representative conclusion for this particular material structure. Furthermore, future work could include the respective balance of plant for each structure.

While the use of the hybrid LCA methodology was chosen to ensure that the system boundary employed in this study was complete, a level of subjectivity on the part of the modeller is imparted through the decision of which missing inputs are added to the SCEnAT*i* decision support tool. Further work in this area could include a wider, expert audience to reduce the level of subjectivity imparted on the model.

As the NBT SOFC materials are currently under investigation, this work will benefit from further study when the full structure has been completed. Furthermore, should the ESB and/or the NBT structures be commercialised, the industrial processed should be compared to give a more accurate world view of the thermal and electrical energy demands.

5. Conclusions

The main aim of investigating and commercialising novel solid oxide fuel cell (SOFC) material structures is to enable them to function at lower temperatures. This work shows the use of these novel material combinations leads to a reduction in the primary energy requirements when compared with commercial SOFC production materials. This saving is achieved by a reduction in the embedded material energy, while an increase in electrical energy has been shown due to the more complicated manufacturing processes required. Overall, the sodium bismuth titanate intermediate temperature SOFC shows the lowest environmental impact across all of the impacts investigated and therefore provides the most environmentally friendly option for future intermediate temperature SOFCs.

While the intermediate temperature SOFC material structures show a reduction in environmental impact when compared to the commercial SOFC, further improvements could be made within the manufacturing process and materials used.

As the sodium bismuth titanate SOFC materials are currently under investigation, this work will benefit from further study when fuel structures have been completed. Furthermore, should the erbia-stabilised bismuth oxide and/or the sodium bismuth titanate structures be commercialised, the industrial processes should be compared to give a more accurate world view of the thermal and electrical energy demands.

Acknowledgements

This work was financially supported by the Engineering and Physical Sciences Research Council (EPSRC-EP/L017563/1) through the University of Sheffield under the project titled: Substitution and Sustainability in Functional Materials and Devices.

Appendix

Life cycle inventories of the material requirements for each of the three SOFC material structures studied in this work. See Tables A1–A3.

Table A1
LCI of the commercial SOFC structure (material inputs adapted from [8]), including the associated GWP 100a impact.

Component	Material	Composition	kg/100 kW	GWP 100a impact
Anode	NiO-YSZ	NiO	68.88	837.44
		YSZ	54.12	1218.61
		Isopropanol	28.29	49.55
		PVA	8.61	17.79
		Methyl methacrylate (binder)	6.16	41.30
		Ethylene glycol (plasticiser)	9.86	18.53
		Trichloroethylene (solvent)	43.10	20.08
		Ethanol (solvent)	43.10	28.94
Electrolyte	YSZ	ZrO_2	1.85	8.92
		Y_2O_3	0.29	4.67
		Ethanol	0.75	0.50
		Elthylcellulose	0.01	0.03
		Polyvinyl butyral	0.02	0.05
		Methyl methacrylate (binder)	0.11	0.72
		Ethylene glycol (plasticiser)	0.17	0.32
		Trichloroethylene (solvent)	0.75	0.35
		Ethanol (solvent)	0.75	0.50
Cathode	LSM-YSZ	Lanthanum oxide	3.82	60.49
		Strontium nitrate	2.48	3.38
		Mn_3O_4	1.35	2.67
		PEG (plasticiser)	1.03	1.93
		Graphite	0.79	0.03
		PVA (binder)	0.44	0.91
		Water	2.93	0.004
		YSZ	2.63	59.11
		Ethylcellulose	0.01	0.05
		Terpineol	0.17	0.32
		Ethylene glycol diethyl ether (solvent)	1.58	2.97
		Ethanol (solvent)	3.68	2.47

Table A2
LCI inventory of the NBT SOFC [12], including the associated GWP 100a impact.

Component	Material	Composition	kg/100 kW	GWP 100a impact
Anode	NiO-GDC	NiO	10.94	133.04
		CeGdO	5.89	218.74
		Solsperse	3.87	7.28
		Toluene	3.87	6.83
		Ethyl alcohol	3.87	2.60
		Di-n butyl phthalate	1.35	2.53
		polyethylene glycol	1.35	2.53
		polyvinyl butral	1.18	2.44
Electrolyte	Sr-NBT	Na_2CO_3	0.06	0.01
		Bi_2O_3	0.25	5.58
		$SrCO_3$	0.01	0.01
		TiO_2	0.19	1.47
		Isopropanol	0.12	0.20
Cathode	LSM-YSZ	Lanthanum oxide	3.82	60.49
		Strontium nitrate	2.48	3.38
		Mn_3O_4	1.35	2.67
		PEG (plasticiser)	1.03	1.93
		Graphite	0.79	0.03
		PVA (binder)	0.44	0.91
		Water	2.93	0.004
		YSZ	2.63	59.11
		Ethylcellulose	0.01	0.05
		Terpineol	0.17	0.32
		Ethylene glycol diethyl ether (solvent)	1.58	2.97
		Ethanol (solvent)	3.68	2.47

Table A3
LCI of the ESB SOFC [6], including the associated GWP 100a impact.

Component	Material	Composition	kg/100 kW	GWP 100a impact
Anode	NiO-GDC	NiO	10.94	133.04
		CeGdO	5.89	218.74
		Solsperse	3.87	7.28
		Toluene	3.87	6.83
		Ethyl alcohol (ethanol)	3.87	2.60
		Di-n butyl phthalate	1.35	2.53
		polyethylene glycol	1.35	2.53
		polyvinyl butral	1.18	2.44
AFL	GDC	GDC	0.03	0.01
		Ethanol	0.003	0.002
Electrolyte 2	GDC	GDC	0.34	0.72
		Solsperse	0.08	0.15
		Ethanol	0.08	0.05
		Di-n butyl phthalate	0.03	0.05
		polyvinyl butral	0.02	0.05
Electrolyte 1	ESB	ER_2O_3	0.03	0.54
		Bi_2O_3	0.14	2.97
		Ethanol	0.04	0.03
Cathode	ESB-BRO7	Bi_2O_3	4.90	107.67
		$RuO_2{\cdot}XH_2O$	2.80	61.85
		ESB	5.13	309.77
		Ethanol	2.95	1.98
		Isopropanol	2.95	5.16

References

[1] Ibn-Mohammed T. Application of mixed-mode research paradigms to the building sector: a review and case study towards decarbonising the built and natural environment. Sustain Cities Soc 2017;35:692–714.
[2] Singhal SC. Solid oxide fuel cells. Electrochem Soc Interface 2007;16:41.
[3] Irshad M, Siraj K, Raza R, Ali A, Tiwari P, Zhu B, et al. A brief description of high temperature solid oxide fuel cell's operation, materials, design, fabrication technologies and performance. Appl Sci (Switzerland) 2016;6.
[4] Brett DJL, Atkinson A, Brandon NP, Skinner SJ. Intermediate temperature solid oxide fuel cells. Chem Soc Rev 2008;37:1568–78.
[5] Su C, Chen Y, Wang W, Ran R, Shao Z, Diniz da Costa JC, et al. Fuel strategy for carbon deposition mitigation in solid oxide fuel cells at intermediate temperatures. Environ Sci Technol 2014;48:7122–7.
[6] Wachsman ED, Lee KT. Lowering the temperature of solid oxide fuel cells. Science 2011;334:935–9.
[7] Ivers-Tiffée E, Weber A, Herbstritt D. Materials and technologies for SOFC-components. J Eur Ceram Soc 2001;21:1805–11.
[8] Lee YD, Ahn KY, Morosuk T, Tsatsaronis G. Environmental impact assessment of a solid-oxide fuel-cell-based combined-heat-and-power-generation system. Energy 2015;79:455–66.
[9] Sun C, Hui R, Roller J. Cathode materials for solid oxide fuel cells: a review. J Solid State Electrochem 2010;14:1125–44.
[10] Tarancón A. Strategies for lowering solid oxide fuel cells operating temperature. Energies 2009;2:1130.
[11] Jacobson AJ. Materials for solid oxide fuel cells. Chem Mater 2010;22:660–74.
[12] Yang F, Zhang H, Li L, Reaney IM, Sinclair DC. High ionic conductivity with low degradation in a-site strontium-doped nonstoichiometric sodium bismuth titanate perovskite. Chem Mater 2016;28:5269–73.
[13] Ibn-Mohammed T, Koh LSC, Reaney IM, Acquaye A, Wang D, Taylor S, et al. Hybrid life cycle assessment and supply chain environmental profile evaluations of lead-based (lead zirconate titanate) versus lead-free (potassium sodium niobate) piezoelectric ceramics. Energy Environ Sci 2016;9:3495–520. 10.1039/C6EE02429G.
[14] Ibn-Mohammed T, Koh S, Reaney I, Sinclair D, Mustapha K, Acquaye A, et al. Are lead-free piezoelectrics more environmentally friendly? MRS Commun 2017:1–7.
[15] Mehmeti A, McPhail SJ, Pumiglia D, Carlini M. Life cycle sustainability of solid oxide fuel cells: From methodological aspects to system implications. J Power Sources 2016;325:772–85.
[16] Strazza C, Del Borghi A, Costamagna P, Traverso A, Santin M. Comparative LCA of methanol-fuelled SOFCs as auxiliary power systems on-board ships. Appl Energy 2010;87:1670–8.
[17] Nease J, Adams Ii TA. Comparative life cycle analyses of bulk-scale coal-fueled solid oxide fuel cell power plants. Appl Energy 2015;150:161–75.
[18] Nease J, Adams TA. Life cycle analyses of bulk-scale solid oxide fuel cell power plants and comparisons to the natural gas combined cycle. Can J Chem Eng 2015;93:1349–63.
[19] Buchgeister J. Comparison of sophisticated life cycle impact assessment methods for assessing environmental impacts in a LCA study of electricity production. In: Proceedings of the 25th international conference on efficiency, cost, optimization and simulation of energy conversion systems and processes, ECOS 2012; 2012. p. 15–26.
[20] Benveniste G, Pucciarelli M, Torrell M, Kendall M, Tarancón A. Life cycle assessment of microtubular solid oxide fuel cell based auxiliary power unit systems for recreational vehicles. J Cleaner Prod 2017;165:312–22.
[21] Stambouli AB, Traversa E. Solid oxide fuel cells (SOFCs): a review of an environmentally clean and efficient source of energy. Renew Sustain Energy Rev 2002;6:433–55.
[22] ISO 14040:2006 environmental management- life cycle assessment- principles and framework. International Organization for Standardization; 2006.
[23] Rebitzer G, Ekvall T, Frischknecht R, Hunkeler D, Norris G, Rydberg T, et al. Life cycle assessment: Part 1: Framework, goal and scope definition, inventory analysis, and applications. Environ Int 2004;30:701–20. https://doi.org/10.1016/j.envint.2003.11.005.
[24] Crawford RH. Validation of a hybrid life-cycle inventory analysis method. J Environ Manage 2008;88:496–506. https://doi.org/10.1016/j.jenvman.2007.03.024.
[25] Ahmed A, Hassan I, Ibn-Mohammed T, Mostafa H, Reaney IM, Koh LS, et al. Environmental life cycle assessment and techno-economic analysis of triboelectric nanogenerators. Energy Environ Sci 2017;10:653–71.
[26] Acquaye AA, Wiedmann T, Feng K, Crawford RH, Barrett J, Kuylenstierna J, et al. Identification of 'carbon hot-spots' and quantification of GHG intensities in the biodiesel supply chain using hybrid LCA and structural path analysis. Environ Sci Technol 2011;45:2471–8. https://doi.org/10.1021/es103410q.
[27] Wiedmann T, Suh S, Feng K, Lenzen M, Acquaye A, Scott K, et al. Application of hybrid life cycle approaches to emerging energy technologies – the case of wind power in the UK. 2011;45:5900-7 10.1021/es2007287.
[28] Ibn-Mohammed T, Koh SCL, Reaney IM, Acquaye A, Schileo G, Mustapha K, et al. Perovskite solar cells: An integrated hybrid lifecycle assessment and review in comparison with other photovoltaic technologies. Renew Sustain Energy Rev 2017;80:1321–44.
[29] Ibn-Mohammed T, Greenough R, Taylor S, Ozawa-Meida L, Acquaye A. Integrating economic considerations with operational and embodied emissions into a decision support system for the optimal ranking of building retrofit options. Build Environ 2014;72:82–101.
[30] Ibn-Mohammed T. Retrofitting the built environment: an economic and environmental analysis of energy systems. Cambridge: Scholars Publishing; 2017.
[31] Oppon E, Acquaye A, Ibn-Mohammed T, Koh L. Modelling multi-regional ecological exchanges: The case of UK and Africa. Ecol Econ 2018;147:422–35.
[32] Acquaye A, Feng K, Oppon E, Salhi S, Ibn-Mohammed T, Genovese A, et al. Measuring the environmental sustainability performance of global supply chains: A multi-regional input-output analysis for carbon, sulphur oxide and water footprints. J Environ Manage 2017;187:571–85.
[33] Pearce JM, Johnson SJ, Grant GB. 3D-mapping optimization of embodied energy of transportation. Resour Conserv Recycl 2007;51:435–53.
[34] Acquaye A, Ibn-Mohammed T, Genovese A, Afrifa GA, Yamoah FA. Oppon EJEJoOR. A Quantitative Model for Environmentally Sustainable Supply Chain Performance Measurement 2018;269:188–205.
[35] Koh SCL, Genovese A, Acquaye AA, Barratt P, Rana N, Kuylenstierna J, et al. Decarbonising product supply chains: design and development of an integrated evidence-based decision support system – the supply chain environmental analysis

tool (SCEnAT). Int J Prod Res 2013;51:2092–109. https://doi.org/10.1080/00207543.2012.705042.
[36] Nagashima S, Uchiyama Y, Okajima K. Hybrid input–output table method for socioeconomic and environmental assessment of a wind power generation system. Appl Energy 2017;185:1067–75. https://doi.org/10.16/j.apenergy.2016.01.018.
[37] Suh S, Lenzen M, Treloar GJ, Hondo H, Horvath A, Huppes G, et al. System boundary selection in life-cycle inventories using hybrid approaches. Environ Sci Technol 2004;38:657–64.
[38] Lake A, Acquaye A, Genovese A, Kumar N, Koh SCL. An application of hybrid life cycle assessment as a decision support framework for green supply chains. Int J Prod Res 2015;53:6495–521. https://doi.org/10.1080/00207543.2014.951092.
[39] Peters J, Buchholz D, Passerini S, Weil M. Life cycle assessment of sodium-ion batteries. Energy Environ Sci 2016;9:1744–51.
[40] Steubing B, Wernet G, Reinhard J, Bauer C, Moreno-Ruiz E. The ecoinvent database version 3 (part II): analyzing LCA results and comparison to version 2. Int J Life Cycle Assess 2016;21:1269–81. https://doi.org/10.007/s11367-016-1109-6.
[41] Ecoinvent. http://www.ecoinvent.org/ accessed 19/09/2017.
[42] Geisler G, Hofstetter TB, Hungerbühler K. Production of fine and speciality chemicals: procedure for the estimation of LCIs. Int J Life Cycle Assess 2004;9:101–13. https://doi.org/10.1007/bf02978569.
[43] Lee KR, Choi SH, Kim J, Lee HW, Lee JH. Viable image analyzing method to characterize the microstructure and the properties of the Ni/YSZ cermet anode of SOFC. J Power Sources 2005;140:226–34.
[44] Juhl M, Primdahl S, Manon C, Mogensen M. Performance/structure correlation for composite SOFC cathodes. J Power Sources 1996;61:173–81.
[45] Chen XJ, Khor KA, Chan SH, Yu LG. Influence of microstructure on the ionic conductivity of yttria-stabilized zirconia electrolyte. Mater Sci Eng, A 2002;335:246–52.
[46] Ding J, Liu J. An anode-supported solid oxide fuel cell with spray-coated yttria-stabilized zirconia (YSZ) electrolyte film. Solid State Ionics 2008;179:1246–9.
[47] Ahn JS, Yoon H, Lee KT, Camaratta MA, Wachsman ED. Performance of IT-SOFC with $Ce_{0.9}Gd_{0.1}O_{1.95}$ functional layer at the interface of $Ce_{0.9}Gd_{0.1}O_{1.95}$ electrolyte and Ni-$Ce_{0.9}Gd_{0.1}O_{1.95}$ anode. Fuel Cells 2009;9:643–9.
[48] Ahn JS, Pergolesi D, Camaratta MA, Yoon H, Lee BW, Lee KT, et al. High-performance bilayered electrolyte intermediate temperature solid oxide fuel cells. Electrochem Commun 2009;11:1504–7.
[49] Ahn JS, Camaratta MA, Pergolesi D, Lee KT, Yoon H, Lee BW, et al. Development of high performance ceria/bismuth oxide bilayered electrolyte SOFCs for lower temperature operation. J Electrochem Soc 2010;157:B376–82.
[50] Camaratta M, Wachsman E. High-performance composite $Bi_2Ru_2O_7$ – $Bi_{1.6}Er_{0.4}O_3$ cathodes for intermediate-temperature solid oxide fuel cells. J Electrochem Soc 2008;155:B135–42.
[51] Li M, Zhang H, Cook SN, Li L, Kilner JA, Reaney IM, et al. Dramatic influence of a-site nonstoichiometry on the electrical conductivity and conduction mechanisms in the perovskite oxide $Na_{0.5}Bi_{0.5}TiO_3$. Chem Mater 2015;27:629–34.
[52] Ahn JS, Omar S, Yoon H, Nino JC, Wachsman ED. Performance of anode-supported solid oxide fuel cell using novel ceria electrolyte. J Power Sources 2010;195:2131–5.
[53] Ibn-Mohammed T, Greenough R, Taylor S, Ozawa-Meida L, Acquaye A. Operational vs. embodied emissions in buildings—A review of current trends. Energy Build 2013;66:232–45.
[54] Ravindra K, Bencs L, Van Grieken R. Platinum group elements in the environment and their health risk. Sci Total Environ 2004;318:1–43.
[55] Smith L, Ibn-Mohammed T, Koh SCL, Reaney IM. Life cycle assessment and environmental profile evaluations of high volumetric efficiency capacitors. Appl Energy 2018;220:496–513.
[56] Guo J, Baker AL, Guo H, Lanagan M, Randall CA. Cold sintering process: A new era for ceramic packaging and microwave device development. J Am Ceram Soc 2017;100:669–77.
[57] Ibn-Mohammed T, Reaney IM, Koh SCL, Acquaye A, Sinclair DC, Randall CA, et al. Life cycle assessment and environmental profile evaluation of lead-free piezoelectrics in comparison with lead zirconate titanate. J Eur Ceram Soc 2018.
[58] Walker H, Di Sisto L, McBain D. Drivers and barriers to environmental supply chain management practices: lessons from the public and private sectors. J Purchasing Supply Manage 2008;14:69–85. https://doi.org/10.1016/j.pursup.2008.01.007.
[59] Northey S, Haque N, Mudd G. Using sustainability reporting to assess the environmental footprint of copper mining. J Cleaner Prod 2013;40:118–28.
[60] Anttila A, Pukkala E, Aitio A, Rantanen T, Karjalainen S. Update of cancer incidence among workers at a copper/nickel smelter and nickel refinery. Int Arch Occup Environ Health 1998;71:245–50. https://doi.org/10.1007/s004200050276.
[61] Lundberg M. Environmental analysis of zirconium alloy production. Uppsala: University; 2011.
[62] Acero AP, Rodriguez C, Ciroth A. Green Delta. 2014 http://www.openlca.org/wp-content/uploads/2016/08/LCIA-METHODS-v.1.5.5.pdf.
[63] Thiers R, Graydon W, Beamish FE. Analytical methods for ruthenium. Anal Chem 1948;20:831–7.
[64] Brenan JM. The platinum-group elements: “Admirably adapted” for science and industry. Elements 2008;4:227–32.
[65] Bossi T, Johnson Matthey JG. The environmental profile of platinum group metals. Technol Rev 2017;61:111–21.
[66] Report of the Ad hoc Working Group on defining critical raw materials “Report on Critical Raw Materials for the EU”. In: Commission E, editor. May 2014.
[67] Hoenderdaal S, Tercero Espinoza L, Marscheider-Weidemann F, Graus W. Can a dysprosium shortage threaten green energy technologies? Energy 2013;49:344–55. https://doi.org/10.1016/j.energy.2012.10.043.
[68] Talens Peiró L, Villalba Méndez G. Material and energy requirement for rare earth production. JOM 2013;65:1327–40. https://doi.org/10.007/s11837-013-0719-8.
[69] Weng Z, Haque N, Mudd GM, Jowitt SM. Assessing the energy requirements and global warming potential of the production of rare earth elements. J Cleaner Prod 2016;139:1282–97.